

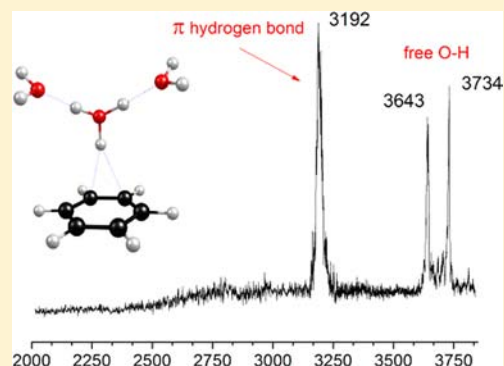
IR Spectroscopy of Protonation in Benzene–Water Nanoclusters: Hydronium, Zundel, and Eigen at a Hydrophobic Interface

Timothy C. Cheng, Biswajit Bandyopadhyay, Jonathan D. Mosley, and Michael A. Duncan*

Department of Chemistry, University of Georgia, Athens, Georgia 30602, United States

S Supporting Information

ABSTRACT: The structure of ions in water at a hydrophobic interface influences important processes throughout chemistry and biology. However, experiments to measure these structures are limited by the distribution of configurations present and the inability to selectively probe the interfacial region. Here, protonated nanoclusters containing benzene and water are produced in the gas phase, size-selected, and investigated with infrared laser spectroscopy. Proton stretch, free OH, and hydrogen-bonding vibrations uniquely define protonation sites and hydrogen-bonding networks. The structures consist of protonated water clusters binding to the hydrophobic interface of neutral benzene via one or more π -hydrogen bonds. Comparison to the spectra of isolated hydronium, zundel, or eigen ions reveals the inductive effects and local ordering induced by the interface. The structures and interactions revealed here represent key features expected for aqueous hydrophobic interfaces.



INTRODUCTION

The accommodation of water at hydrophobic interfaces has far-reaching implications for chemistry and biology, influencing processes such as protein folding, membrane formation, enzyme–substrate binding, and the performance of hydrogen fuel cells.^{1–3} The hydrogen-bonding network of water is believed to restructure in the vicinity of such an interface; unraveling the details of this reorganization represents a significant challenge for experiment and theory.^{4–11} In many important situations, ionization of water adds complexity to these interfaces. Simulations and experiments suggest that hydronium ions are locally enriched near an interface, whereas hydroxide ions are relatively depleted here.^{12–15} Again, the local structure and dynamics are extremely difficult to measure directly. Techniques such as sum frequency generation are surface sensitive^{4,5,8–11,15} but suffer from the distribution of bulk configurations sampled. New insights into hydrogen-bonding structures and solvation have been provided by infrared spectroscopy of size-selected protonated water clusters in the gas phase.^{16–25} Unlike solution measurements, these experiments select the composition of an ion and the number of solvent molecules interacting with it. High-level computational studies have complemented these experiments.^{26–28} We describe here such a study of protonated water–benzene clusters containing several of each solvent molecule. This system reveals fascinating aspects of the structures and interactions present at a model hydrophobic interface.

The structural motifs of protonated water are well known.^{29–32} In addition to hydronium (H_3O^+), the zundel ion (H_3O_2^+) has a proton equally shared between two water molecules and the eigen ion (H_3O_4^+) has hydronium solvated

symmetrically by three water molecules. These structures are implicated as important intermediates, informing the discussion of protonation and proton transfer dynamics in many situations. Each has been characterized with spectroscopy in the gas phase.^{16–23,33} In particular, new selected-ion infrared spectroscopy studies and computational work have documented the infrared signatures for various protonated water clusters, $\text{H}^+(\text{H}_2\text{O})_n$, up to and including the clathrate cages that form in the $n > 20$ size range.^{16–25} Mixed clusters containing protonated water interacting with other solvents have also been described, focusing on the proton stretching vibration at low frequencies and its dependence on relative proton affinities.³⁴ Likewise, the protonated benzene ion (also known as benzenium) has also been studied with selected-ion infrared spectroscopy, and it has a spectrum distinctly different from that of protonated water.^{35,36} Small neutral (bz)(H_2O)_n clusters have been studied,^{37,38} as have (bz)(H_2O)_n⁺ cations,^{39,40} but there is only limited data for protonated benzene–water mixtures.^{41,42} Here, we explore the infrared spectroscopy and structures of $\text{H}^+(\text{H}_2\text{O})_n(\text{bz})_m$ clusters, where $n, m = 1–4$. Benzene has a higher proton affinity (750.4 kJ/mol) than water (691.0 kJ/mol)⁴³ and is more polarizable, while water forms more stable hydrogen-bonding networks. The competition for proton binding sites and differential solvation in these systems exhibit many of the key features of aqueous interfaces.

Received: April 20, 2012

Published: July 18, 2012

EXPERIMENTAL SECTION

Cluster ions for these experiments are produced using a pulsed discharge source employing needle electrodes. The needles are mounted with a 1 mm gap and centered on the gas flow emanating from a pulsed valve (General Valve, series 9) about 2–3 mm downstream from the valve opening. One electrode is grounded, and the other is pulsed at a voltage of -1000 V for a period of $10 \mu\text{s}$ in the middle of the $300 \mu\text{s}$ gas pulse. Water is added to the system in the form of a few drops inserted into the gas lines, while benzene vapor in equilibrium with a liquid sample at 0°C is entrained into the rare gas flow. The balance of the beam gas is 30% hydrogen and 70% argon at a total pressure of about 10 atm. Hydrogen enhances ionization via the production of H_3^+ cations followed by proton transfer to water or benzene.

Ions and their clusters are transported through the instrument in the form of a neutral plasma molecular beam.⁴⁴ After passing through a skimmer, the contents of the beam are sampled into the mass spectrometer with pulsed acceleration fields. A specially designed reflectron time-of-flight mass spectrometer⁴⁵ is employed to mass-analyze the cluster ions and to select them by size. Selected ions are excited with a tunable optical parametric oscillator laser system (LaserVision), pumped by a Nd:YAG laser (Spectra Physics PRO-230), covering the infrared range of $600\text{--}4500 \text{ cm}^{-1}$.

Because the density of these mass-selected ions is too low for absorption measurements, we use photodissociation to measure their spectroscopy. Unfortunately, smaller ions with bond energies greater than the energy of the IR photons do not dissociate upon infrared excitation. To investigate these species, we employ the method of messenger atom pre-dissociation or “tagging”,^{16,46–49} whereby the $\text{H}^+(\text{H}_2\text{O})_n(\text{benzene})_m$ ion of interest is produced in a mixed complex with argon, i.e., $\text{H}^+(\text{H}_2\text{O})_n(\text{benzene})_m\text{Ar}$. Resonant excitation of these complexes, followed by intramolecular vibrational relaxation (IVR), leads to elimination of argon. This mass change is detected with the mass spectrometer as a function of energy to record the spectrum. For many of the larger ions, we are not able to achieve efficient argon tagging. However, these ions have gradually weaker bonding, and many of them dissociate by losing solvent molecules. We find experimentally that benzene elimination occurs from these systems rather than water. We therefore record this mass change to measure the spectra of the larger ions. Unfortunately, the binding energy of benzene is such that we cannot detect signals in the lower frequency range for these ions.

The structures, bonding, and infrared spectra of these benzene–water complexes are studied computationally with density functional theory (DFT) using the B3LYP functional, as implemented in the Gaussian03 program suite.⁵⁰ Selected smaller ions are also studied at the MP2, B97-D, and B2PLYP-D levels for comparison to the DFT results. The 6-311+G(d,p) basis set was employed throughout these computations. The results of the computational studies for each ion–molecule complex are presented below and in the Supporting Information (SI). For comparison to the measured infrared spectra, the computed frequencies are scaled by a factor of 0.9575 for DFT/B3LYP and 0.9368 for MP2. These factors were derived by comparing the computed vibrations for the O–H stretches of H_2O and H_3O^+ to those measured experimentally.

RESULTS AND DISCUSSION

Figure 1 shows a comparison of the infrared spectra measured for the hydronium ion (top), protonated benzene (bottom), and the 1:1 protonated benzene–water complex (middle). The isolated hydronium ion has been studied previously with high resolution infrared absorption spectroscopy; its O–H stretch vibrations occur at $3390/3491$ (ν_1 symmetric stretch) and $3519/3536 \text{ cm}^{-1}$ (ν_3 asymmetric stretch; both are inversion doublets).³³ Tagging with one argon atom is not sufficient to enable IR photodissociation, but attachment of two argons make this possible. The spectrum at higher frequency contains a free O–H stretch (3540 cm^{-1}) and two more red-shifted

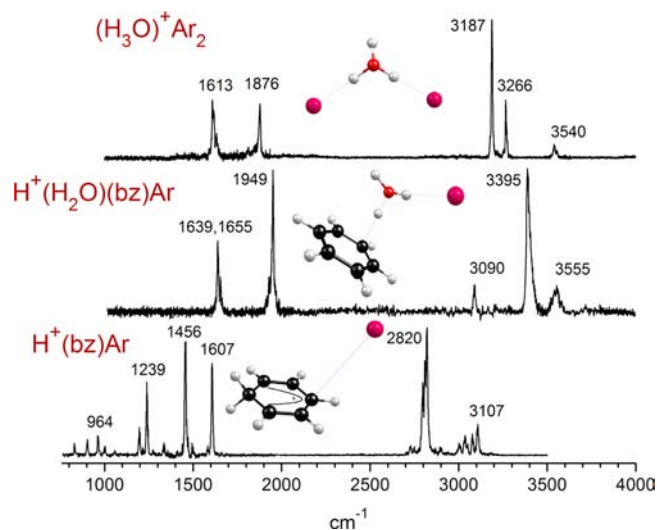


Figure 1. Vibrational spectrum of the benzene– H^+ –water complex (center) compared to those of the hydronium ion (top) and protonated benzene (bottom). The vibrations of the mixed complex are more like those of hydronium.

bands assigned to the symmetric (3187 cm^{-1}) and asymmetric (3266 cm^{-1}) stretches of the OH's bound to argon. The free OH band is close to the position of the asymmetric stretch in free hydronium, but the other vibrations are red-shifted by the presence of the argons. In the lower frequency region, the scissors bend of water occurs at 1613 cm^{-1} and a combination band between this bend and a water torsion occurs at 1876 cm^{-1} .⁵¹ The protonated benzene cation has a quite different spectrum with no O–H stretches.^{35,36} σ protonation produces a CH_2 group on the ring and the charge is delocalized in the aromatic ring opposite this. Its spectrum includes the strong band at 2820 cm^{-1} , corresponding to the overlapping symmetric and asymmetric stretches of the CH_2 , and the scissors bend of this group at 1239 cm^{-1} ; strong activity is also induced in the ring skeleton modes at 1456 and 1607 cm^{-1} . Bands near 3107 cm^{-1} arise from the aromatic C–H stretches and/or overtones and combinations of lower frequency vibrations. Benzene itself has a well-known multiplet of bands here from a Fermi resonance,⁵² and a similar effect likely produces the multiplet pattern is seen here. Because the vibrational patterns are so different for hydronium versus protonated benzene, the spectrum of the mixed benzene–water complex (center) can be compared to these to determine its essential character. As shown, $\text{H}^+(\text{H}_2\text{O})(\text{bz})$ has free OH bands and a bending mode like hydronium, but no CH_2 bands near 2820 cm^{-1} and no activity in the skeletal ring modes or CH_2 bends characteristic of protonated benzene. From the comparisons to the isolated ions, therefore, it is clear that the mixed protonated system is more like hydronium–benzene than it is like benzenium–water. The vibration at 1949 cm^{-1} can be identified as the shared proton stretch; its frequency lies at almost exactly the value predicted using the analysis of Johnson and co-workers for a mixed component proton-bound dimer with a proton affinity difference (ΔPA) of about 60 kJ/mol .³⁴

Theory is highly problematic for this system, with quite different results obtained from DFT and MP2 methods (see SI). Because the energetics are likely more reliable with the MP2 calculations, we number the three low-lying isomers a, b, and c, identified by their relative energies at this level. MP2

Table 1. Computed Binding Energies and Relative Energies (in kcal/mol, with Respect to the Most Stable Isomer) of $H^+(H_2O)_n(bz)_mAr_x$ Complexes^a

complex	DFT/B3LYP		MP2	
	ΔE	B.E.	ΔE	B.E.
$H^+(H_2O)(bz)$, isomer a (hydronium–benzene; free OH's over ring)	+3.5	25.0 (bz)	0.0	28.7 (bz)
$H^+(H_2O)(bz)$, isomer b (hydronium–benzene; free OH's away from ring)	+3.8	24.8 (bz)	+0.7	26.2 (bz)
$H^+(H_2O)(bz)$, isomer c (benzenium–water)	0	11.4 (H_2O)	+6.2	13.6 (H_2O)
$H^+(H_2O)(bz)Ar$, isomer a	+1.9	1.9 (Ar)	0.0	3.5 (Ar)
$H^+(H_2O)(bz)Ar$, isomer b	+2.2	1.9 (Ar)	<i>b</i>	<i>b</i>
$H^+(H_2O)(bz)Ar$, isomer c	0.0	0.3 (Ar)	+7.8	1.9 (Ar)
$H^+(H_2O)_2(bz)$, isomer a	0.0	15 (bz)	0.0	18.7 (bz)
$H^+(H_2O)_2(bz)$, isomer b	+13.7	9.4 (bz)	+24.3	9.6 (bz)
$H^+(H_2O)_2(bz)Ar$, isomer a (argon “cis” to benzene)	0.0	1.1(Ar)	0.0	2.7 (Ar)
$H^+(H_2O)_2(bz)Ar$, isomer b (argon “trans” to benzene)	+0.3	0.8 (Ar)	+1.5	1.2 (Ar)
$H^+(H_2O)_3(bz)$, isomer a	0.0	11.4 (bz)		
$H^+(H_2O)_3(bz)$, isomer b	+21.0	7.2 (bz)		
$H^+(H_2O)_4(bz)$, isomer a	0.0	7.0 (bz)		
$H^+(H_2O)_4(bz)$, isomer b	+25.0	12.2 (bz)		
$H^+(H_2O)(bz)_2$, isomer a	0.0	16.0 (bz)		
$H^+(H_2O)(bz)_2$, isomer b	+6.6	5.8 (bz)		
$H^+(H_2O)(bz)_2Ar$	0.0	1.0 (Ar)		
$H^+(H_2O)_2(bz)_2$, isomer a-cis	0.0	10.7 (bz)		
$H^+(H_2O)_2(bz)_2$, isomer a-trans	+1.4	9.3 (bz)		
$H^+(H_2O)_2(bz)_2Ar$, isomer a-cis	0.0	0.6 (Ar)		
$H^+(H_2O)_2(bz)_2Ar$, isomer a-trans	+0.9	1.2 (Ar)		
$H^+(H_2O)_3(bz)_2$	0.0	7.5 (bz)		
$H^+(H_2O)(bz)_3$, isomer a	0.0	10.6 (bz)		
$H^+(H_2O)(bz)_3$, isomer b	+12.6	4.7 (bz)		
$H^+(H_2O)_2(bz)_3$	0.0	7.7 (bz)		
$H^+(H_2O)_2(bz)_4$	0.0	5.7 (bz)		

^aCalculations are done with the MP2 and/or B3LYP levels of theory with the 6-311+G(d,p) basis set. Energies are not ZPVE or BSSE corrected. The binding energies (B.E.) are for elimination of the ligand/solvent species indicated in parentheses. ^bDid not converge with argon.

finds the hydronium–benzene structure (isomer a) at lower energy, while DFT/B3LYP finds a benzenium–water structure (isomer c) lying lower in energy (~3.5 kcal/mol) than the hydronium–benzene structure. A second hydronium–benzene isomer (b) has the hydronium free OH's pointing away from the benzene ring rather than over it as in isomer a. This isomer lies at intermediate energy for the MP2 calculations, but is the least stable of the three with DFT/B3LYP. These energy differences change only slightly when argon is attached. These energetics are presented in Table 1 for clusters with and without argon. The DFT structures for the hydronium–benzene isomers a and b have the proton connecting with the benzene ring at a single carbon atom site, whereas the MP2 structures for these have the proton bridging two ring carbons. It is well known that MP2 energetics are more reliable than DFT for these kinds of systems, and that DFT has trouble with hydrogen bonds.⁵³ Because of these issues with DFT/B3LYP versus MP2 calculations, we also examined the 1:1 complex with the dispersion-corrected functionals B97-D and B2PLYP-D. These results are provided in the SI. Both of these functionals find the same energetic ordering for the isomers as that found with B3LYP, with similar small energy differences, and both find the hydronium–benzene structure with a single carbon connection, similar to isomers a and b found with B3LYP. There is therefore no apparent improvement in the relative energetics for these isomers with the dispersion-corrected functionals.

The energetic preference for the hydronium–benzene structure reflected in the MP2 calculation agrees with our

spectral analysis discussed above. We have found in the past that, for a given ion–molecule complex structure, DFT/B3LYP (using appropriate scaling) reproduces the vibrational patterns more accurately than MP2, even though its energetics may be less reliable.^{22,36} We find this to be the case here, where the B3LYP spectra are closer to the experiment than MP2, B-97-D, or B2PLYP-D predictions (see SI). Consistent with previous findings for related systems,^{26–28} all of the computational methods have trouble with the shared proton stretch vibration, predicting it higher than it is actually observed. Figure 2 shows that the best agreement with the experiment is found for the B3LYP spectrum of isomer b, whose energy is slightly (0.3 kcal/mol) higher than the most stable isomer a at the MP2 level. This is the hydronium–benzene structure with the free OH's pointed away from the benzene ring. While the other vibrations fit reasonably well with the other methods used here (see SI). Even for the isolated zundel ion, it has been shown that full-dimensional anharmonic theory is required to obtain an accurate picture of the proton stretch vibration.²⁸ Both DFT and MP2 predict significant IR activity in the benzene ring modes for the benzenium–water structure (isomer c), which is not seen. Therefore, although there are some issues with the computations here, the combined picture from theory and experiment is that we have produced the hydronium–benzene complex. We have conducted a similar comparison of DFT and MP2 computations for the $H^+(H_2O)_2(bz)$ complex. Unlike the 1:1 system, here we find good agreement between all methods on the most stable isomeric structures (see Table 1 and SI).

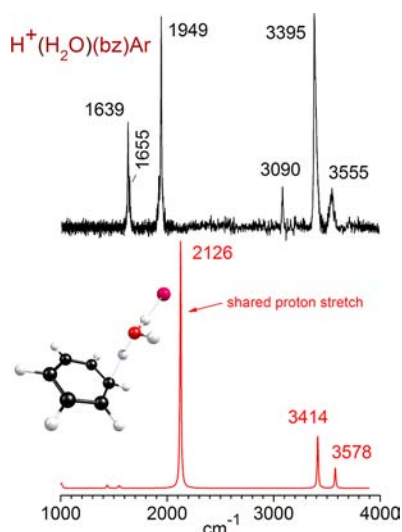


Figure 2. Spectrum of the $\text{H}^+(\text{H}_2\text{O})(\text{bz})\text{Ar}$ complex compared to the predictions of theory at the DFT/B3LYP/6-311+G(d,p) level for the hydronium–benzene isomer b (with hydronium free OH's pointed away from ring). Although this isomer is not predicted to be the lowest in energy, it agrees best with the experimental spectrum.

Because of this, the better performance of DFT/B3LYP for vibrations, and because of the significant sizes of the larger clusters studied, we focus on DFT/B3LYP computations for the remainder of this work.

The $\text{H}^+(\text{H}_2\text{O})(\text{bz})$ complex therefore has its proton on water instead of benzene, even though benzene has a higher proton affinity. This can be rationalized using the electrostatic interactions of nascent solvation in this system. Benzene has a much higher polarizability ($10.74 \times 10^{-24} \text{ cm}^3$) than water ($1.45 \times 10^{-24} \text{ cm}^3$).⁵⁴ Therefore, the charge–induced dipole interaction is enhanced when there is a small charge center on hydronium interacting with the highly polarizable benzene partner. Conversely, the charge on protonated benzene is delocalized in the π system, and its interaction with the dipole of water is less favorable. In a computational study, Fridgen has investigated heterogeneous proton-bound dimers where one component has a strong dipole moment and the higher proton affinity.⁵⁵ In these systems, the shared proton is positioned closer to the species with the lower proton affinity, because this structure enhances the charge–dipole interaction. Johnson and co-workers have confirmed this scenario experimentally for the acetonitrile–water proton-bound dimer.⁵⁶ Although the details are different here (benzene has no dipole moment, but is highly polarizable) the more favorable electrostatic interactions also determine the structure obtained in the benzene–water system.

Figure 3 shows the spectrum for the tagged $\text{H}^+(\text{H}_2\text{O})_2(\text{bz})$ ion (center) compared to that of the protonated water dimer (top), also known as the zundel ion. The zundel ion spectrum has been reported previously^{16–23} and this system has been studied extensively with theory.^{26–28} Its argon-tagged spectrum has four O–H stretches because argon attachment breaks the symmetry. The signature for this ion is the shared proton vibrations, which produce a multiplet of bands with a most intense feature at 1073 cm^{-1} . The water bending mode occurs at 1764 cm^{-1} . The spectrum of $\text{H}^+(\text{H}_2\text{O})_2(\text{bz})$ is similar to this, with three O–H stretches in nearly the same positions, but a fourth band is strongly red-shifted. In the low-frequency region, two bands are shifted to higher frequencies from those in zundel. None of these bands resemble the pattern of

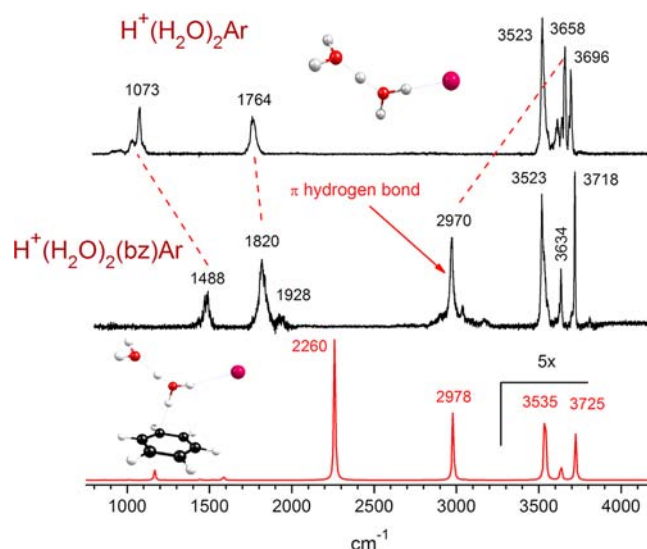


Figure 3. Vibrational spectrum of the $\text{H}^+(\text{H}_2\text{O})_2(\text{bz})\text{Ar}$ complex (center) compared to those of the zundel ion (top) and the most stable zundel–benzene isomer resulting from computations (DFT/B3LYP/6-311+G(d,p) level) (bottom). The mixed complex has characteristic features of the zundel ion, but with noticeable frequency shifts.

protonated benzene. Theory using both DFT and MP2 finds a lowest energy structure with a zundel ion attached to neutral benzene via a π -hydrogen bond. The spectrum predicted for this complex (bottom) reproduces the free O–H stretches (except for their intensities, whose values measured via photodissociation are typically greater than computed for absorption) and shows that the 2970 cm^{-1} band is the O–H stretch of the π -hydrogen bond (for spectra of other isomers see SI). Additional weaker bands near this likely come from the C–H stretch of benzene. The proton stretch predicted at 2260 cm^{-1} is far from any measured bands, consistent with the results obtained previously for the isolated zundel ion.^{17–21} The comparison to theory and to the isolated zundel ion shows that $\text{H}^+(\text{H}_2\text{O})_2(\text{bz})$ has zundel attached to neutral benzene.

The π -hydrogen-bonding vibration at 2970 cm^{-1} reveals the contact point between water and benzene in the $\text{H}^+(\text{H}_2\text{O})_2(\text{bz})$ complex. This kind of vibration has been seen previously for neutral water–benzene clusters³⁸ near $3640\text{--}3650 \text{ cm}^{-1}$ and recently in water–benzene solutions at 3610 cm^{-1} .⁵⁷ Here, this frequency is much lower than the free O–H stretches, and is in the region of hydrogen-bonding bands in pure water clusters. However, it does not have the broad line width seen for these features in protonated water clusters (see below). Other vibrations in this system reveal the effects of polarization and induction remote from this contact point. The proton stretch and water bending modes at 1488 and 1820 cm^{-1} are shifted to higher frequencies compared to their values in the isolated zundel ion. The computed structure (see SI) has the proton shifted closer (about 1.0 \AA) to the water in contact with benzene than it is to the other water (about 1.4 \AA). The OH attached to benzene is polarized, making the oxygen end more negative, which in turn attracts the proton more strongly. The proton shifts closer to oxygen, leading to an asymmetric local environment and higher frequencies. As shown by Johnson and co-workers in a systematic study of proton-bound dimers, asymmetric environments lead to higher frequencies for the proton stretch, consistent with the trend seen here.³⁴ However,

although the proton position is closer to one water than to the other, the spectrum still has the shared-proton vibration characteristic of the zundel species. Shifts to higher frequency also occur for the free OH vibrations of the zundel moiety opposite benzene. The bands at 3634 and 3718 cm^{-1} from the symmetric and asymmetric stretches here are both shifted to higher frequency from their values in zundel. Remarkably, these vibrations are twice-removed from the contact point with benzene. The hydrophobic interface binds zundel, attracts the proton, and induces an overall more rigid structure extending through the hydrogen-bonding network.

Figure 4 shows the spectrum of the $\text{H}^+(\text{H}_2\text{O})_3(\text{bz})$ complex, measured in the mass channel for the elimination of benzene,

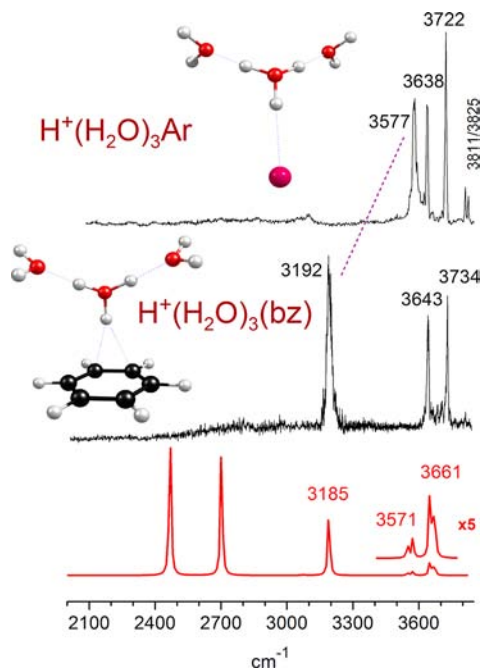


Figure 4. Vibrational spectrum of the $\text{H}^+(\text{H}_2\text{O})_3(\text{bz})$ complex (center) compared to that of the $\text{H}^+(\text{H}_2\text{O})_3$ complex (top) and to the spectrum predicted by theory (DFT/B3LYP/6-311+G(d,p) level) for the most stable isomer (bottom).

compared to that of the $\text{H}^+(\text{H}_2\text{O})_3\text{Ar}$ complex and the predictions of DFT theory. We observe experimentally that photodissociation takes place by the elimination of neutral benzene rather than water. Consistent with this, our computed binding energies are greater for water (21.0 kcal/mol) than they are for benzene (11.4 kcal/mol; 3990 cm^{-1}) (see SI). These computed binding energies from DFT methods are not likely to be quantitative, but apparently the relative values are correct, because we observe benzene elimination rather than water. The actual benzene elimination channel must have a threshold energy below 3192 cm^{-1} where our lowest energy band is detected. Again, theory predicts a structure having the protonated water cluster attached to neutral benzene, and the spectrum is completely consistent with this. The protonated water trimer has a central hydronium-based structure, with water molecules attached to its terminal OH's. Symmetric and asymmetric free O–H stretches (3638 and 3722 cm^{-1}) are detected, and a third O–H stretch is red-shifted to 3577 cm^{-1} because of the attachment of argon. Weak combination bands (O–H stretch + water torsion) appear as a doublet at higher frequency. An intense doublet of hydrogen-bonding symmetric

and asymmetric stretches was predicted by theory for $\text{H}^+(\text{H}_2\text{O})_3\text{Ar}$ near 2500 cm^{-1} but not detected.²² Such “missing” vibrations have also been described for several protonated water clusters having the hydronium moiety imbedded in a hydrogen-bonding network, including most famously the $\text{H}^+(\text{H}_2\text{O})_{21}$ species believed to have a clathrate cage structure.^{22,24} In the small clusters, the hydronium vibrations are believed to be lifetime, broadened beyond the detection limit by rapid IVR,²² whose rate is different for vibrations more strongly coupled to the hydrogen-bonding network. In larger systems such as the 21-mer, it has also been proposed that dynamical sampling of structural configurations other than hydronium occurs at the finite temperature of the experiments.⁵⁸ Similar effects are believed at least in part to cause the broadening of bands associated with other hydrogen-bonding vibrations (see below). In the $\text{H}^+(\text{H}_2\text{O})_3(\text{bz})$ complex here, the two free O–H stretches remain in nearly their same positions, but the third terminal OH binds to benzene, producing a π -hydrogen-bonding band at 3192 cm^{-1} . This band is reproduced nicely by theory. Again, as seen before for the protonated water trimer, two strong hydronium-based vibrations are predicted but not detected. This could be from the IVR effect noted above, but in this case it is more likely a result of the benzene binding energy. The hydronium-based π -hydrogen-bonding band here appears at significantly higher frequency than the one seen for the zundel–benzene complex in Figure 3 (2970 cm^{-1}). As in that system, the free OH vibrations remote from this contact point are also shifted to slightly higher frequencies.

Another example of the long-range influence of the water–benzene interface occurs for the $\text{H}^+(\text{H}_2\text{O})_4(\text{bz})$ cluster, which has the eigen ion interacting at a single contact point with benzene. The isolated eigen spectrum, measured with argon tagging, is compared to that of $\text{H}^+(\text{H}_2\text{O})_4(\text{bz})$ in Figure 5, where the latter is measured by the loss of neutral benzene. Here the binding energy of benzene to the eigen ion is calculated to be about 7.0 kcal/mol (3450 cm^{-1}), but fragmentation signal is detected down to about 2600 cm^{-1} . The eigen ion has symmetric and asymmetric free O–H

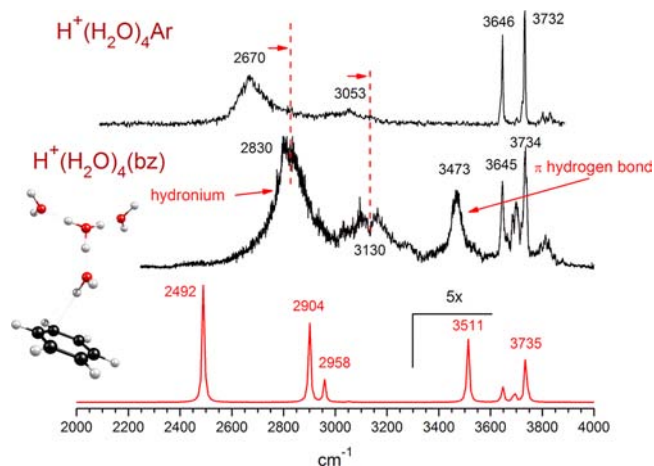


Figure 5. Vibrational spectrum of the $\text{H}^+(\text{H}_2\text{O})_4(\text{bz})$ complex (center) compared to that of the eigen ion (top) and to the most stable eigen–benzene isomer resulting from computations (DFT/B3LYP/6-311+G(d,p) level) (bottom). The mixed complex has characteristic features of the eigen ion, but with noticeable frequency shifts.

stretches at 3646 and 3732 cm^{-1} , and two broad bands at 2670 and 3053 from the symmetric and asymmetric hydrogen-bonding stretches of the central hydronium. $\text{H}^+(\text{H}_2\text{O})_4(\text{bz})$ has these same bands and an additional one at 3473 cm^{-1} arising from the π -hydrogen bond. Unlike the $\text{H}^+(\text{H}_2\text{O})_3(\text{bz})$ complex above, both the free eigen ion and its benzene complex have hydronium vibrations that appear in the spectrum. However, all of these, including also the π -hydrogen-bonding band, are broadened significantly, presumably by the IVR effect noted above. The π -hydrogen-bonding vibration occurs at a much higher frequency than those in either the zundel–benzene complex in Figure 2 or the hydronium–benzene complex in Figure 3. Apparently, as more water molecules are present supporting the hydrogen-bonding network, the frequency of the π -hydrogen-bonding vibration goes up. Additionally, the hydronium bands in the eigen–benzene complex are also shifted to higher frequencies compared to those in the free ion, occurring at 2830 and 3130 cm^{-1} (additional structure on the latter band may come from overlapping benzene C–H stretches). Again, the interface with benzene stiffens the hydrogen-bonding network remote from the contact point. On the other hand, the free O–H stretches opposite benzene are not shifted noticeably. Although the interface extends its influence well into the hydrogen-bonding network, there is eventually a limit to its effect. The spectrum predicted by theory does not match the experimental pattern in the hydrogen-bonding region. The symmetric/asymmetric hydrogen-bonding O–H stretch vibrations opposite benzene (2904 and 2958 cm^{-1}) are predicted to split far apart from the one toward benzene (2492 cm^{-1}). Broadened bands are observed near the higher frequency bands, but not for the lower. It is again conceivable that we have missed the lower component because of the benzene binding energy here, but the similarity to the structure for the isolated eigen ion and its benzene complex in this region is quite strong, suggesting that theory may have overestimated this splitting and/or underestimated the hydrogen-bonded stretch frequencies of hydronium.

Figure 6 shows the spectrum of the $\text{H}^+(\text{H}_2\text{O})_3(\text{bz})_2$ complex, measured in the benzene elimination channel, compared to that predicted by theory for the most stable isomer, whose structure is shown in the inset. Again, because the benzene elimination is measured, the spectrum does not extend to lower frequencies. Surprisingly, this spectrum has several more bands detected in the hydrogen-bonding region than the corresponding monobenzene complex shown in Figure 4. Just from the qualitative appearance of the spectrum, it is apparent that the second benzene causes a significant change in this system. The nature of the change is apparent in the most stable structure predicted for this system, which has the two benzenes binding on opposite ends of a zundel type ion, with the third water binding to the side of the zundel moiety. The second benzene induces a transformation in the system, from one with a hydronium-based core ion for the $\text{H}^+(\text{H}_2\text{O})_3(\text{bz})$ complex to one with a zundel core for $\text{H}^+(\text{H}_2\text{O})_3(\text{bz})_2$. The IR spectrum detected agrees nicely with the spectrum predicted for this system. There are three distinct free OH stretches, corresponding to the symmetric and asymmetric stretches of the external water and the single vibration on one of the zundel waters. Two π -hydrogen-bonding bands are predicted at 3294 and 3467 cm^{-1} and detected at 3295 and 3433 cm^{-1} ; both are broadened significantly. These are assigned to symmetric and asymmetric motions of the two π -hydrogen bonds into benzene. A single OH–water hydrogen-bonding vibration is predicted at 2845

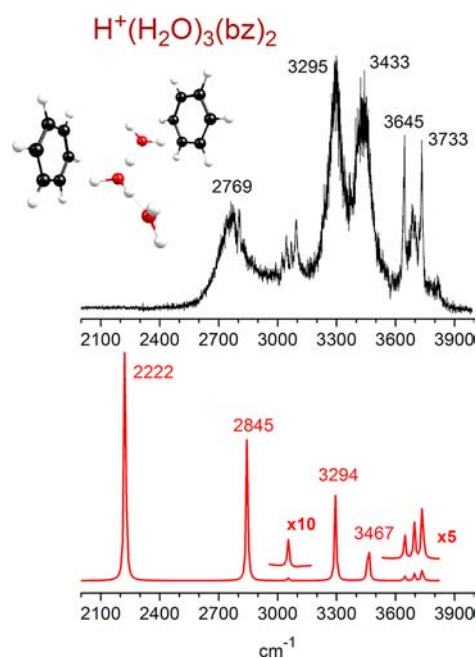


Figure 6. Vibrational spectrum of the $\text{H}^+(\text{H}_2\text{O})_3(\text{bz})_2$ complex compared to that predicted for the most stable isomer resulting from theory.

cm^{-1} and measured at 2769 cm^{-1} , also broadened. A single weak C–H stretching band is predicted near 3100 cm^{-1} , and this is detected as a Fermi multiplet in this same region. Finally, the proton stretch of the zundel moiety is predicted at 2222 cm^{-1} , quite close to where this vibration was predicted for the $\text{H}^+(\text{H}_2\text{O})_2(\text{bz})$ in Figure 3. As in this smaller system, the actual position of the proton stretch is likely at lower frequency, below the region that can be measured here because of the benzene binding energy. In this system then, the benzene positions around the protonated water produce a more symmetric environment, which then favors the symmetric proton binding in the zundel ion. Remarkably, all the hydrogen-bonding motions predicted to be present are in fact detected, and the line widths are comparable for the OH–water versus OH–benzene vibrations.

It is interesting that the two benzenes in this complex prefer to bind to water in the π -hydrogen-bonding configurations rather than to each other. The binding energy of neutral benzene dimer is quite low (2–3 kcal/mol).⁵⁹ Compared to this, the binding energy of benzene on the OH of water in the structure here is about 7.5 kcal/mol. Therefore, it makes sense qualitatively that the second benzene prefers to bind to water rather than to the first benzene. If the benzenium ion were present, the benzenium–benzene interactions would be stronger (dimer bond energy computed to be about 10 kcal/mol),^{60,61} but this favorable interaction is apparently offset by the loss in efficient hydrogen-bonding and water ion–benzene interactions.

To examine the progressive solvation of these ions with benzene, we have examined the set of spectra for the $\text{H}_3\text{O}^+(\text{bz})_m$ species ($m = 0–4$). Theory and spectra for all of these systems indicate that the structures have hydronium interacting with neutral benzenes, as indicated. These spectra are shown in Figure 7. The bottom two traces show hydronium itself without any benzene, and the 1:1 hydronium–benzene complex, as described earlier in Figure 1. These both have free

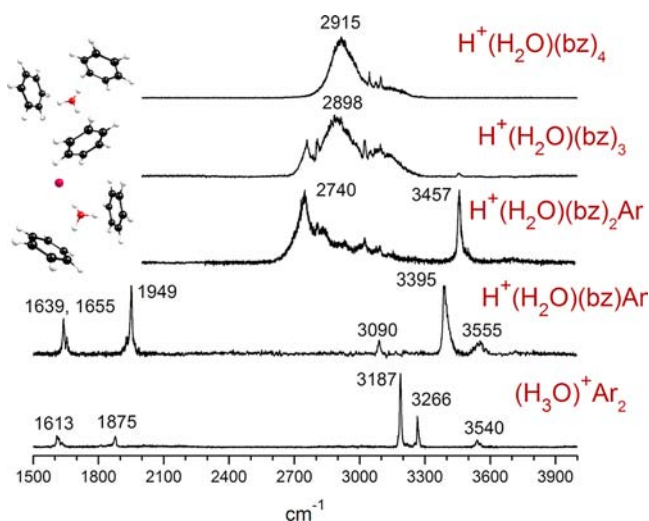


Figure 7. Vibrational spectra of $\text{H}^+(\text{H}_2\text{O})(\text{bz})_{0-4}$ complexes. As benzene encloses the hydronium ion, the frequencies of the π -hydrogen bond increase and the intensities of the free OH bands decrease.

OH vibrations at high frequency, water bends at the lowest frequency, and then the 1:1 complex has a shared proton stretch at 1949 cm^{-1} . The addition of a second benzene for the $\text{H}_3\text{O}^+(\text{bz})_2$ complex induces a dramatic change in the spectrum, consistent with the structure predicted by theory (see Figure S10 in SI), which has hydronium in a double π -hydrogen bond configuration with the two benzenes. Consequently, the shared proton stretch vibration becomes a symmetric/asymmetric π -hydrogen-bonding stretch doublet (unresolved here because of the width), shifted to much higher frequency. The broad band centered near 2740 cm^{-1} is in the range predicted by theory for this doublet, and the free OH (with argon attached) appears at 3457 cm^{-1} . This free OH band is also shifted significantly to higher frequency compared to that in the 1:1 complex. Partial confinement of hydronium by two benzenes therefore results in a much more rigid overall system. This trend continues with the addition of a third benzene, where the computed structure has hydronium completely enclosed within three π -hydrogen bonds to benzene. The symmetric/asymmetric proton stretch doublet predicted (see Figure S11) appears experimentally as a broad feature again, whose center-of-mass is shifted again toward higher frequency. The structure on the blue end of this probably has weak benzene C–H stretch bands superimposed on it. The free OH vibration is essentially gone, consistent with the confinement of hydronium, although there is a slight trace of a band here indicating the survival of a minor concentration of an isomer with a free OH. With the addition of a fourth benzene, the complete confinement of hydronium is assured. There is no trace of the free OH, and the hydronium stretch region appears to have collapsed into a single broad band, but one which is narrower than those for the smaller clusters. In addition to this main broad band, there is a weak multiplet present from the C–H stretch of benzene. The band at 2915 cm^{-1} here represents hydronium in a high-symmetry environment, completely enclosed by benzene. As in the $\text{H}^+(\text{H}_2\text{O})_3(\text{bz})_2$ system above in Figure 6, benzene prefers to bind to water to form stable π -hydrogen bonds, and this leads to a water-templated structure rather than a structure with segregated water and benzene domains. The $\text{H}^+(\text{H}_2\text{O})_3(\text{bz})_4$ system should have one excess benzene molecule binding to the

outside of the system, but we have not pursued theory on this system due to the multiple isomeric structures expected to lie close in energy. We have just completed a study of the clusters of the form $\text{H}^+(\text{bz})_n$ for $n = 2, 3$, where the complexities of such benzene–benzene interactions are described in detail.⁶¹

A final example of structuring at the protonated water–benzene interface is provided in Figure 8 for the

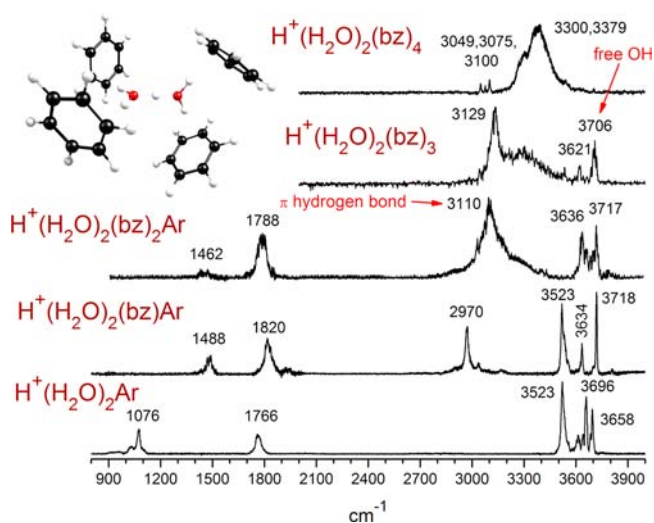


Figure 8. Vibrational spectra of $\text{H}^+(\text{H}_2\text{O})_2(\text{bz})_{0-4}$ complexes. As benzene encloses the zundel ion, the frequencies of the π -hydrogen bond increase and the intensities of the free OH bands decrease.

$\text{H}^+(\text{H}_2\text{O})_2(\text{bz})_m$ ($m = 0-4$) series. Theory and spectral analysis show that these clusters all have the zundel core interacting with progressively more benzene. The $m = 0, 1$ complexes have an argon-on-free OH band at 3523 cm^{-1} that drops out at $m = 2$ because the argon attachment position changes. The $m = 1, 2$ complexes have similar spectra; the characteristic low-frequency bands identify the zundel moiety (as in Figure 3), and the π -hydrogen-bond bands (2970 and 3110 cm^{-1} , respectively) define the contact point(s) with benzene. There is a simpler two-band symmetric/asymmetric free O–H stretch pattern after this. We were unable to tag with argon for the larger complexes, and these spectra are measured via the loss of benzene. Its stronger binding precludes detection of signal in the lower frequency region. The key aspects of these spectra are the trends in the π -hydrogen bond and the free O–H stretches. As benzene encloses zundel, the π -hydrogen bond shifts to higher frequency, corresponding to a more rigid structure, in the same way seen above for enclosure of hydronium. In the $m = 4$ species, this shift uncovers the benzene C–H stretches near 3100 cm^{-1} . The free OH bands gradually decrease in intensity and then drop out at $m = 4$, confirming that zundel is completely enclosed. This complex has four π -hydrogen bonds with benzene on each of the terminal OH positions in a structure resembling a reverse micelle. Remarkably, as in the $\text{H}^+(\text{H}_2\text{O})_3(\text{bz})_{2,3}$ complexes discussed above, zundel templates benzene maximizing the interfacial contacts; there is no evidence for a segregated benzene–water structure. Because there are four π -hydrogen bonds here, the overall system is even more rigid than it was for the enclosed hydronium, and the resulting O–H stretches are at even higher frequency (3300 instead of 2915 cm^{-1}).

The cluster growth dynamics suggested for these various protonated water–benzene clusters are quite fascinating.

Although many low-lying isomeric structures are predicted by theory, the clusters detected all have some form of water cluster ion core surrounded by neutral benzenes. There is no evidence for benzenium ions solvated by water, even though these species are sometimes close in energy. We mentioned above that some of this can be rationalized by the favorable ion-induced dipole interactions for water ions next to the highly polarizable benzene(s). However, it is still surprising that each of the spectra observed can be assigned to just a single isomer. With the possible exception of the $\text{H}^+(\text{H}_2\text{O})(\text{bz})_3$ complex (see Figure S11 in SI), there is no compelling evidence for the coexistence of more than one isomer in any of these systems. Coexisting isomers have been detected recently in several other related cluster systems.^{62–64} In at least some of these, high barriers exist to interconversion, preventing less stable isomers from rearranging into more stable forms. Since this behavior is not observed here, it seems that there must not be any large activation barriers for rearrangements in the present benzene–water systems. This makes good sense, because many of the isomers in question differ only by the position of protons, which are easily mobile. However, another possible factor in the larger clusters that are not tagged is a bias in our measurements toward weakly bonded external ligands. In some of the benzenium-based complexes, the external ligand that would be eliminated by IR excitation is a water molecule with relatively strong binding energy. These isomers are computed to be significantly less stable. However, even if they were formed they would be harder to detect because of the higher external ligand bonding energies.

Like the pure protonated water ions studied previously, these mixed benzene–water systems exhibit unusual vibrational dynamics. As in other shared proton systems,^{24,26–28} the proton stretch vibrations here at low frequencies are not described well by harmonic theory. Some combination bands are indicated, but most of the bands can be assigned to vibrational fundamentals. Various bands assigned to OH and π -hydrogen-bonding vibrations are significantly broader than those assigned to free OH or CH vibrations. This broadening cannot be caused by the overlap of bands for multiple isomers, since the other patterns in the spectra confirm the presence of just a single isomer. Instead, these line widths indicate different vibrational dynamics for hydrogen-bonding vibrations compared to those of other modes. As we have discussed elsewhere,²² the most likely explanation is lifetime broadening from the increased rate of IVR for vibrations more strongly connected to the hydrogen-bonding network. This was also seen for pure protonated water clusters.^{22,24} In some of the larger clusters here (i.e., Figures 7 and 8), at least part of the line broadening may arise from the more elevated temperature of the ions. Larger ions grow later in the expansion than smaller ones, experience fewer cooling collisions, and have greater heat capacity to cool. However, thermal effects should affect all the vibrations more or less equally. Many of the clusters with broadened bands in the hydrogen-bonding region have sharp bands in the free O–H or C–H stretch region, and then a temperature effect is less likely.

The structural patterns in these systems are compelling. The core ion in every case is a protonated water cluster interacting with benzene, whose structure is essentially the same as that for the isolated species. Small changes in bond distances and angles occur, and vibrations shift in interesting ways, but the protonated water structures appear to be quite robust. The other recurring theme is the occurrence of π -hydrogen bonds at

the contact point(s) between these water cluster ions and the neutral benzene(s). Such π -hydrogen bonds have been seen previously,^{38,57} but in these systems they form the interfacial contact here in every system. Their frequency positions and line widths vary widely depending on the local environment, providing an unanticipated range of behavior. Surprisingly, in sharp contrast to the related shared proton vibrations, theory seems to handle the frequencies of these π -hydrogen bond vibrations quite nicely.

In general, these systems provide a serious challenge for theory. Beginning with the 1:1 complex, we found a widely different behavior for the energetics of hydronium–benzene versus benzenium–water structures. In the larger clusters, the preference for water-based ions became clearer, but the descriptions of shared proton vibrations was somewhat problematic throughout. From our spectral analysis and comparison to the known spectra for protonated water ions, we are able to identify the essential character of these clusters, but this task would have been much more difficult if it were based only on computational results. In the work so far, we focused on DFT/B3LYP calculations because of the perceived better performance for vibrational spectra. Dispersion-corrected functionals such as B97-D and B2PLYP-D were tried for the smaller clusters. Although the energies found with these methods may be more reliable than those with B3LYP, the vibrational spectra resulting from these are much worse in comparison with the experiment. It would be worthwhile to investigate all of the clusters here with a variety of methods to further elucidate the relative energies of the isomers, but unfortunately our experiment does not measure these energetics except indirectly through photodissociation thresholds. A more comprehensive computational study might also identify additional isomeric structures that we did not find. However, the spectral analysis here is internally consistent and is consistent with the spectra measured previously for the protonated water ions, neutral benzene, and the benzenium ion. Because of this, we do not expect the basic story here to change significantly with better theory. An additional useful approach might be to study these clusters with other methods such as collision-induced dissociation (CID) to check the predicted dissociation thresholds for different structures. In this regard, Hauptert and Wenthold have recently completed a CID study of the $\text{H}^+(\text{benzene})(\text{water})$ ion.⁶⁵ The threshold in this work could only be explained with a hydronium–benzene structure, consistent with our present conclusions. Additional CID studies of larger clusters would also be informative.

CONCLUSIONS

A variety of small ion–molecule complexes containing protonated benzene–water mixtures have been produced at low temperature, mass-selected, and studied with infrared photodissociation spectroscopy. The isomeric structures and corresponding infrared spectra have also been investigated with computational chemistry. Because protonated water clusters and protonated benzene have been studied before with similar methods, the spectra of the mixed systems can also be compared to the well-known patterns of the pure-component ions. All of these mixed complexes are found to contain protonated water clusters bound to neutral benzene as a result of favorable ion–benzene electrostatic interactions. A key feature throughout these systems is the π -hydrogen bond which forms the interfacial contact point(s) between water ions and benzene. Hydronium, zundel and eigen ions are strongly bound

to this interface and their vibrations away from the contact point(s) become more rigid from the resulting inductive forces running through the hydrogen-bonding network. Induced frequency shifts extend through multiple network bonds remote from the contact point. The π -hydrogen-bond vibration shifts initially to lower frequency compared to free O–H stretches, but then to higher frequency as additional contact points develop in larger aggregates. The strong π -hydrogen-bonding that forms in these systems between water ions and benzene may be just the kind of interaction responsible for the enrichment of water ions near bulk hydrophobic interfaces.^{12–15} These data may also be relevant for recent experiments on vibrational dynamics at bulk hydrophobic interfaces,^{9–11} where it is found that orientational relaxation of the hydrogen-bonding network slows considerably compared to the bulk solution.^{9–11} The vibrational shifts to higher frequencies seen in these clusters near their interfaces, and the corresponding more rigid hydrogen-bonding network here, would act to inhibit structural rearrangements, thus slowing the dynamics. The water–water and water–benzene interactions in these systems outweigh benzene–benzene interactions so that benzene aggregates around water rather than segregating into an “oil-like” domain. Remarkably, these small water–benzene clusters seem to display many of the essential physical characteristics of bulk hydrophobic interfaces.

■ ASSOCIATED CONTENT

■ Supporting Information

Complete ref 50; computational results (geometries, frequencies, binding energies, IR spectral comparisons) for each of the structures considered in this work. This material is available free of charge via the Internet at <http://pubs.acs.org>.

■ AUTHOR INFORMATION

Corresponding Author

maduncan@uga.edu

Notes

The authors declare no competing financial interest.

■ ACKNOWLEDGMENTS

This research is supported by the National Science Foundation through grant no. CHE-0956025.

■ REFERENCES

- (1) Ball, P. *Chem. Rev.* **2008**, *108*, 74–108.
- (2) Berne, B. J.; Weeks, J. D.; Zhou, R. *Annu. Rev. Phys. Chem.* **2009**, *60*, 85–103.
- (3) Zhong, D.; Pal, S. K.; Zewail, A. H. *Chem. Phys. Lett.* **2011**, *503*, 1–11.
- (4) (a) Scatena, L. F.; Brown, M. G.; Richmond, G. L. *Science* **2001**, *292*, 908–912. (b) Hore, D. K.; Walker, D. S.; Richmond, G. L. *J. Am. Chem. Soc.* **2008**, *130*, 1800–1801.
- (5) (a) Gopalakrishnan, S.; Liu, D.; Allen, H. C. *Chem. Rev.* **2006**, *106*, 1155–1175. (b) Chen, X.; Hua, W.; Huang, Z.; Allen, H. C. *J. Am. Chem. Soc.* **2010**, *132*, 11336–11342. (c) Hua, W.; Chen, X.; Allen, H. C. *J. Phys. Chem. A* **2011**, *115*, 6233–6238.
- (6) Chowdhary, J.; Ladanyi, B. M. *J. Phys. Chem. B* **2009**, *113*, 4045–4053.
- (7) Johnson, M. E.; Malardier-Jugroot, C.; Murarka, R. K.; Head-Gordon, T. *J. Phys. Chem. B* **2009**, *113*, 4082–4092.
- (8) Eftekhari-Bafrooei, A.; Borguet, E. *J. Am. Chem. Soc.* **2010**, *132*, 3756–3761.
- (9) (a) Bakulin, A. A.; Pshenichnikov, M. S.; Bakker, H. J.; Petersen, C. *J. Phys. Chem. A* **2011**, *115*, 1821–1829. (b) Zhang, Z.; Piatkowski, L.; Bakker, H. J.; Bonn, M. *J. Chem. Phys.* **2011**, *135*, 021101/1–3.
- (10) Fayer, M. D. *Acc. Chem. Res.* **2012**, *45*, 3–14.
- (11) (a) Bakker, H. J.; Skinner, J. L. *Chem. Rev.* **2010**, *110*, 1498–1517. (b) Skinner, J. L.; Pieniazek, P. A.; Gruenbaum, S. M. *Acc. Chem. Res.* **2012**, *45*, 93–100.
- (12) (a) Vácha, R.; Horinek, D.; Berkowitz, M. L.; Jungwirth, P. *Phys. Chem. Chem. Phys.* **2008**, *10*, 4975–4980. (b) Jagoda-Cwiklik, B.; Cwiklik, L.; Jungwirth, P. *J. Phys. Chem. A* **2011**, *115*, 5881–5886. (c) Vácha, R.; Rick, S. W.; Jungwirth, P.; de Beer, A. G. F.; de Aguiar, H. B.; Samson, J.-S.; Roke, S. *J. Am. Chem. Soc.* **2011**, *133*, 10204–10210.
- (13) Iuchi, S.; Chen, H.; Paesani, F.; Voth, G. A. *J. Phys. Chem. B* **2009**, *113*, 4017–4030.
- (14) Wick, C. D.; Cummings, O. T. *Chem. Phys. Lett.* **2011**, *503*, 161–166.
- (15) (a) Petersen, P. B.; Saykally, R. J. *J. Phys. Chem. A* **2005**, *109*, 7976–7980. (b) Petersen, P. B.; Saykally, R. J. *Chem. Phys. Lett.* **2008**, *458*, 255–261.
- (16) (a) Yeh, L. I.; Okumura, M.; Myers, J. D.; Price, J. M.; Lee, Y. T. *J. Chem. Phys.* **1989**, *91*, 7319–7330. (b) Okumura, M.; Yeh, L. I.; Myers, J. D.; Lee, Y. T. *J. Phys. Chem.* **1990**, *94*, 3416–3427. (c) Jiang, J.-C.; Wang, Y.-S.; Chang, H.-C.; Lin, S. H.; Lee, Y. T.; Niedner-Schatteburg, G.; Chang, H.-C. *J. Am. Chem. Soc.* **2000**, *122*, 1398–1410.
- (17) Asmis, K. R.; Pivonka, N. L.; Santambrogio, G.; Brummer, M.; Kaposta, C.; Neumark, D. M.; Wöste, L. *Science* **2003**, *299*, 1375–1377.
- (18) Fridgen, T. D.; McMahon, T. B.; MacAleese, L.; Lemaire, J.; Maitre, P. *J. Phys. Chem. A* **2004**, *108*, 9008–9010.
- (19) (a) Headrick, J. M.; Bopp, J. C.; Johnson, M. A. *J. Chem. Phys.* **2004**, *121*, 11523–11526. (b) Diken, E. G.; Headrick, J. M.; Roscioli, J. R.; Bopp, J. C.; Johnson, M. A.; McCoy, A. B. *J. Phys. Chem. A* **2005**, *109*, 1487–1490. (c) Hammer, N. I.; Diken, E. G.; Roscioli, J. R.; Johnson, M. A.; Myshakin, E. M.; Jordan, K. D.; McCoy, A. B.; Huang, X.; Bowman, J. M.; Carter, S. *J. Chem. Phys.* **2005**, *122*, 244301/1–10. (d) McCunn, L. R.; Roscioli, J. R.; Johnson, M. A.; McCoy, A. B. *J. Phys. Chem. B* **2008**, *112*, 321–327. (e) McCunn, L. R.; Roscioli, J. R.; Elliott, B. M.; Johnson, M. A.; McCoy, A. B. *J. Phys. Chem. A* **2008**, *112*, 6074–6078. (f) Olesen, S. G.; Guasco, T. L.; Roscioli, J. R.; Johnson, M. A. *Chem. Phys. Lett.* **2011**, *509*, 89–95.
- (20) Headrick, J. M.; Diken, E. G.; Walters, R. S.; Hammer, N. I.; Christie, R. A.; Cui, J.; Myshakin, E. M.; Duncan, M. A.; Johnson, M. A.; Jordan, K. D. *Science* **2005**, *308*, 1765–1769.
- (21) Chang, H.-C.; Wu, C.-C.; Kuo, J.-L. *Int. Rev. Phys. Chem.* **2005**, *24*, 553–578.
- (22) Douberly, G. E.; Walters, R. S.; Cai, J.; Jordan, K. D.; Duncan, M. A. *J. Phys. Chem. A* **2010**, *114*, 4570–4579.
- (23) Mizuse, K.; Fujii, A. *Phys. Chem. Chem. Phys.* **2011**, *13*, 7098–7104.
- (24) Shin, J.-W.; Hammer, N. I.; Diken, E. G.; Johnson, M. A.; Walters, R. S.; Jaeger, T. D.; Duncan, M. A.; Christie, R. A.; Jordan, K. D. *Science* **2004**, *304*, 1137–1140.
- (25) Miyazaki, M.; Fujii, A.; Ebata, T.; Mikami, N. *Science* **2004**, *304*, 1134–1137.
- (26) (a) Huang, X.; Cho, H. M.; Carter, S.; Ojamae, L.; Bowman, J. M.; Singer, S. J. *J. Phys. Chem. A* **2003**, *107*, 7142–7155. (b) Dai, J.; Bacic, Z.; Huang, X.; Carter, S.; Bowman, J. M. *J. Chem. Phys.* **2003**, *119*, 6571–6580. (c) Huang, X.; Braams, B. J.; Bowman, J. M. *J. Chem. Phys.* **2005**, *122*, 044308/1–12. (d) McCoy, A. B.; Huang, X.; Carter, S.; Landeweer, M. Y.; Bowman, J. M. *J. Chem. Phys.* **2005**, *122*, 061101/1–4. (e) Kaledin, M.; Kaledin, A. L.; Bowman, J. M. *J. Phys. Chem. A* **2006**, *110*, 2933–2939. (f) Kaledin, M.; Kaledin, A. L.; Bowman, J. M.; Ding, J.; Jordan, K. D. *J. Phys. Chem. A* **2009**, *113*, 7671–7677.
- (27) (a) Singh, N. J.; Park, M.; Min, S. K.; Suh, S. B.; Kim, K. S. *Angew. Chem., Int. Ed.* **2006**, *45*, 3795–3800. (b) Park, M.; Shin, I.; Singh, N. J.; Kim, K. S. *J. Phys. Chem. A* **2007**, *111*, 10692–10702.

- (28) (a) Vendrell, O.; Gatti, F.; Meyer, H.-D. *Angew. Chem., Int. Ed.* **2007**, *46*, 6918–6921. (b) Vendrell, O.; Gatti, F.; Lauvergnat, D.; Meyer, H.-D. *J. Chem. Phys.* **2007**, *127*, 184302/1–17. (c) Vendrell, O.; Gatti, F.; Meyer, H.-D. *J. Chem. Phys.* **2007**, *127*, 184303/1–10. (g) Vendrell, O.; Meyer, H.-D. *Phys. Chem. Chem. Phys.* **2008**, *10*, 4692–4703. (d) Vendrell, O.; Gatti, F.; Meyer, H.-D. *Angew. Chem., Int. Ed.* **2009**, *48*, 352–355. (e) Vendrell, O.; Brill, M.; Gatti, F.; Lauvergnat, D.; Meyer, H.-D. *J. Chem. Phys.* **2007**, *130*, 234305/1–13. (f) Vendrell, O.; Gatti, F.; Meyer, H.-D. *J. Chem. Phys.* **2009**, *131*, 034308/1–9.
- (29) Eigen, M. *Angew. Chem., Int. Ed.* **1964**, *3*, 1–19.
- (30) Zundel, G. *Adv. Chem. Phys.* **2000**, *111*, 1–217.
- (31) Agmon, N. *Chem. Phys. Lett.* **1995**, *244*, 456–462.
- (32) Cukierman, S. *Biochim. Biophys. Acta* **2006**, *1757*, 876–885.
- (33) (a) Begemann, M. H.; Gudeman, C. S.; Pfaff, J.; Saykally, R. J. *Phys. Rev. Lett.* **1983**, *51*, 554–557. (b) Begemann, M. H.; Saykally, R. J. *J. Chem. Phys.* **1985**, *82*, 3570–3579. (c) Tang, J.; Oka, T. *J. Mol. Spectrosc.* **1999**, *196*, 120–130.
- (34) Roscioli, J. R.; McCunn, L. R.; Johnson, M. A. *Science* **2007**, *316*, 249–254.
- (35) Solcà, N.; Dopfer, O. *Angew. Chem., Int. Ed.* **2002**, *41*, 3628–3631.
- (36) Douberly, G. E.; Ricks, A. M.; Duncan, M. A. *J. Phys. Chem. A* **2008**, *112*, 4869–4874.
- (37) Suzuki, S.; Green, P. G.; Bumgarner, R. E.; Dasgupta, S.; Goddard, W. A., III; Blake, G. A. *Science* **1992**, *257*, 942–945.
- (38) (a) Grotch, A. J.; Zwier, T. S. *J. Chem. Phys.* **1992**, *96*, 3388–3401. (b) Pribble, R. N.; Zwier, T. S. *Science* **1994**, *265*, 75–79. (c) Gruenloh, C. J.; Carney, J. R.; Arrington, C. A.; Zwier, T. S.; Fredericks, S. Y.; Jordan, K. D. *Science* **1997**, *276*, 1678–1681.
- (39) (a) Solcà, N.; Dopfer, O. *Chem. Phys. Lett.* **2001**, *347*, 59–64. (b) Solcà, N.; Dopfer, O. *J. Phys. Chem. A* **2003**, *107*, 4046–4055.
- (40) (a) Miyazaki, M.; Fujii, A.; Ebata, T.; Mikami, N. *Phys. Chem. Chem. Phys.* **2003**, *5*, 1137–1148. (b) Miyazaki, M.; Fujii, A.; Ebata, T.; Mikami, N. *J. Phys. Chem. A* **2004**, *108*, 8269–8272. (c) Miyazaki, M.; Fujii, A.; Ebata, T.; Mikami, N. *J. Phys. Chem. A* **2004**, *108*, 10656–10660.
- (41) Solcà, N.; Dopfer, O. *Chem.—Eur. J.* **2003**, *9*, 3154–3163.
- (42) Chaudhuri, C.; Wu, C.-C.; Jiang, J.-C.; Chang, H.-C. *Aust. J. Chem.* **2004**, *57*, 1153–1156.
- (43) Hunter, E. P.; Lias, S. G. Proton Affinity Evaluation In *NIST Chemistry WebBook*, NIST Standard Reference Database Number 69; Linstrom, P. J., Mallard, W. G., Eds.; National Institute of Standards and Technology: Gaithersburg, MD, February 2008; <http://webbook.nist.gov>.
- (44) Duncan, M. A. *Annu. Rev. Phys. Chem.* **1997**, *48*, 69–93.
- (45) Cornett, D. S.; Peschke, M.; LaiHing, K.; Cheng, P. Y.; Willey, K. F.; Duncan, M. A. *Rev. Sci. Instrum.* **1992**, *63*, 2177–2186.
- (46) Ebata, T.; Fujii, A.; Mikami, N. *Int. Rev. Phys. Chem.* **1998**, *17*, 331–361.
- (47) Bieske, E. J.; Dopfer, O. *Chem. Rev.* **2000**, *100*, 3963–3998.
- (48) Robertson, W. H.; Johnson, M. A. *Annu. Rev. Phys. Chem.* **2003**, *54*, 173–213.
- (49) Duncan, M. A. *Int. Rev. Phys. Chem.* **2003**, *22*, 407–435.
- (50) Frisch, M. J. et al. *Gaussian 03*, Revision B.02; Gaussian, Inc.: Pittsburgh, PA, 2003.
- (51) Olesen, S. G.; Gausco, T. L.; Weddle, G. H.; Hammerum, S.; Johnson, M. A. *Mol. Phys.* **2010**, *108*, 1191–1197.
- (52) Shimanouchi, T. Molecular Vibrational Frequencies. *NIST Chemistry WebBook*, NIST Standard Reference Database Number 69; Linstrom, P. J., Mallard, W. G., Eds.; National Institute of Standards and Technology: Gaithersburg, MD, February 2008; <http://webbook.nist.gov>.
- (53) Cohen, A. J.; Mori-Sánchez, P.; Yang, W. *Chem. Rev.* **2012**, *112*, 289–320.
- (54) Lide, D. R., Ed. *Handbook of Chemistry and Physics*, 79th ed.; CRC Publishing: New York, 1999.
- (55) Fridgen, T. D. *J. Phys. Chem. A* **2006**, *110*, 6122–6128.
- (56) Gardenier, G. H.; Roscioli, J. R.; Johnson, M. A. *J. Phys. Chem. A* **2008**, *112*, 12022–12026.
- (57) Gierszal, K. P.; Davis, J. G.; Hands, M. D.; Wilcox, D. S.; Slipchenko, L. V.; Ben-Amotz, D. *J. Phys. Chem. Lett.* **2011**, *2*, 2930–2933.
- (58) Iyengar, S. S.; Petersen, M. K.; Day, T. J. F.; Burnham, C. J.; Teige, V. E.; Voth, G. A. *J. Chem. Phys.* **2005**, *123*, 084309/1–9.
- (59) Sherrill, C. D.; Takatani, T.; Hohenstein, E. G. *J. Phys. Chem. A* **2009**, *113*, 10146–10159.
- (60) Jaeger, H. M.; Schaefer, H. F.; Hohenstein, E. G.; Sherill, C. D. *Comp. Theor. Chem.* **2011**, *973*, 47–52.
- (61) Bandyopadhyay, B.; Cheng, T. C.; Wheeler, S. E.; Duncan, M. A. *J. Phys. Chem. A* **2012**, *116*, 7065–7073.
- (62) Elliot, B. M.; Relph, R. A.; Roscioli, J. R.; Bopp, J. C.; Gardenier, G. H.; Guasco, T. L.; Johnson, M. A. *J. Chem. Phys.* **2008**, *129*, 094303/1–6.
- (63) Douberly, G. E.; Ricks, A. M.; Schleyer, P. v. R.; Duncan, M. A. *J. Chem. Phys.* **2008**, *128*, 021102/1–4.
- (64) Ricks, A. M.; Douberly, G. E.; Schleyer, P. v. R.; Duncan, M. A. *J. Chem. Phys.* **2010**, *132*, 051101/1–4.
- (65) Haubert, L. J.; Wenthold, P. G. *J. Phys. Chem. A*, submitted.